

ON THE ORIGIN OF THE INNER STRUCTURE OF HALOS

Alberto Manrique, Andreu Raig, Eduard Salvador-Sole¹, Teresa Sanchis
and Jose Marta SolanesDepartament d'Astronomia i Meteorologia, Universitat de Barcelona,
Marti Franques 1, E-08028 Barcelona, SpainAlberto Manrique@ub.es, arraig@ub.es, eduard@ub.es, tsanchis@ub.es, and jsolanes@ub.es
Draft version May 22, 2019

ABSTRACT

We calculate by means of the Press-Schechter formalism the density profile developed by dark matter halos during accretion, i.e., the continuous aggregation of small clumps. We find that the shape of the predicted profile is similar to that shown by halos in high-resolution cosmological simulations. Furthermore, the mass-concentration relation is correctly reproduced at any redshift in all the hierarchical cosmologies analyzed, except for very large halo masses. The role of major mergers, which can cause the rearrangement of the halo structure through violent relaxation, is also investigated. We show that, as a result of the boundary conditions imposed by the matter continuously infalling into the halo during the violent relaxation process, the shape of the density profile emerging from major mergers is essentially identical to the shape the halo would have developed through pure accretion. This result explains why, according to high-resolution cosmological simulations, relaxed halos of a given mass have the same density profile regardless of whether they have had a recent merger or not, and why both spherical infall and hierarchical assembly lead to very similar density profiles. Finally, we demonstrate that the density profile of relaxed halos is not affected either by the capture of clumps of intermediate mass.

Subject headings: cosmology: theory | dark matter | galaxies: halos, structure, formation

1. introduction

The dominant dark component of matter in the universe is clustered in bound halos which form the skeleton of all astronomical objects of cosmological interest, from dwarf galaxies to rich galaxy clusters. The determination of the inner structure of such halos has been addressed both analytically and by numerical simulations.

The analytical approach to this problem was pioneered by Gunn & Gott (1972), who adopted the simplifying assumption that halos grow through spherical infall, i.e., the monolithic collapse of a density fluctuation of isotropically distributed, cold, collisionless matter in an otherwise homogeneous expanding universe. This allowed them to derive the density profile resulting from self-similar initial conditions in an Einstein-de Sitter universe up to the onset of shell crossing. The effects of shell crossing and of adopting more and more realistic initial conditions were addressed and the whole treatment was refined in a series of subsequent papers (Gott 1975; Gunn 1977; Fillmore & Goldreich 1984; Bertschinger 1985; Homan & Shaham 1985; Ryden & Gunn 1987; Ryden 1988; Zaroubi & Homan 1993; Henriksen & Widrow 1999; Lokas 2000; Lokas & Homan 2000; DelPopolo et al. 2000; Engineer, Kanekar, & Padmanabhan 2000; Nusser 2001).

According to these studies, after the collapse of some initial seed, a stationary regime is reached, the so-called secondary infall, in which the system grows inside-out. This is the consequence of the fact that the orbital period of particles in any shell is smaller than the characteristic time of secular variation of their apapsis (or turn-around radius) owing to shell crossing of the infalling layers. Accordingly, 1) particles spend most of the time near the apapsis of their orbits, which makes their time-averaged radius close

to that value, and 2) shell crossing gently alters the initial apapsis (corresponding to maximum expansion) of layers, making them contract by a monotonously varying factor of order two and, hence, with no apapsis crossing. This is an important result since, provided the infall rate of matter is known, the inside-out growth condition completely determines the halo density profile. Much progress has been achieved in the last twenty years in the modeling of halo mass growth. In particular, the extended Press-Schechter (PS) model (Press & Schechter 1974; Bower 1991; Bond et al. 1991; Lacey & Cole 1993) makes accurate predictions on the rate at which halos increase their mass in hierarchical cosmologies (Lacey & Cole 1994). Unfortunately, in such cosmologies, halos develop from small to large scales by successive aggregations rather than through smooth spherical infall.

There are different ways in the literature to refer to the mass assembly process. Some authors call each individual aggregation event "merger" (e.g., Bower 1991; Bond et al. 1991; Lacey & Cole 1993), while others use the word "accretion" to refer to their cumulative effect (e.g., Wechsler et al. 2002, hereafter W02; Zhao et al. 2003). In N-body or Monte Carlo simulations, it is also usual to use the words "merger" and "accretion" depending on whether the captured clumps are resolved or not, respectively (e.g., Somerville & Kolatt 1999). On the other hand, if one is only interested in the mass growth of halos, the distinction between "major" and "minor" mergers or "fast" and "slow" accretion is not important as it represents solely an arbitrary classification of captures according to the mass increase they produce. However, in dealing with the structural and kinematical effects of aggregation events on a given halo, such a distinction is crucial.

When a halo captures a much less massive clump its

¹ CERN for Astrophysics, Particle Physics, and Cosmology, Universitat de Barcelona, Marti Franques 1, E-08028 Barcelona, Spain

structure is essentially unperturbed while, in the case that both objects have comparable masses, the system is brought far from equilibrium and violently relaxes again (Lynden-Bell 1967), thus losing the memory of the previous history. The new equilibrium state is characterized by a normal distribution of the velocities of the different constituents similar to that yielded by two-body relaxation, although independent of the particle mass. Consequently, were halos unperturbed after any such dramatic event, they would end up as spherical systems with uniform, isotropic velocity dispersion. For this reason, halos are often modeled as isotropic, monomassive, isothermal spheres (e.g., King 1972; Shapiro, Iliev, & Raga 1999). However, halos are not isolated systems and they continue collecting matter during violent relaxation, which makes the final state difficult to predict (e.g., Saslaw 1987). In addition, the frontier between minor and major captures is rather blurred and intermediate captures have their own specific dynamical effects. The associated clumps undergo substantial dynamical friction and spiral to the halo center rather than move along stable orbits. Then, the density distribution is neither unaltered nor completely rearranged, but becomes a little cuspy at the halo center.

The situation is therefore quite complicated and difficult to implement in an analytical model. For this reason some authors have turned to numerical experiments. Navarro, Frenk, & White (1996; 1997, hereafter NFW) found, through N-body simulations of several hierarchical cosmologies, that the spherically averaged density profile of current halos of a wide range of masses is always well fitted by the simple analytical expression

$$\rho(r) = \frac{c r_s^3}{r(r_s + r)^2}; \quad (1)$$

hereafter referred to as the NFW profile. In equation (1), r is the radial distance to the halo center, and r_s and c are the halo scale radius and characteristic density, respectively. The latter two parameters are related to each other and to the mass M of the halo through the condition that the average density within the virial radius R of the system is equal to f times ρ_u , with f a constant factor independent of mass and ρ_u some characteristic density of the universe. NFW adopted ρ_u equal to the critical density ρ_{crit} , and $f = 200$, although ρ_u equal to the mean cosmological density and other values of f are also often adopted.

On the other hand, Cole & Lacey (1997) showed that the spherically averaged, locally isotropized, velocity dispersion profile $\sigma(r)$ is well fitted by the solution of the Jeans equation for hydrostatic equilibrium and negligible rotation

$$\sigma^2(r) \frac{d \ln \sigma^2}{d \ln r} + \frac{d \ln \sigma^2}{d \ln r} = \frac{3 G M(r)}{r}; \quad (2)$$

where G is the gravitational constant, $\rho(r)$ the density profile given in equation (1) and $M(r)$ the corresponding mass profile, for the boundary condition of null pressure at infinity.

These results have been extensively confirmed (e.g., Tormen, Bouchet, & White 1997; Huzz, Jain, & Steinmetz 1999b; Bullock et al. 2001). There is only some controversy on the exact slope of the density profile at very small radii (Moore et al. 1998; Jing & Suto 2000; Fukushige & Makino 2001; Klypin et al. 2001; Power et al. 2003), the most af-

fected by the limited resolution of simulations. Nonetheless, in spite of the substantial progress in our knowledge on the inner structure of halos ordered by N-body simulations, the physical origin of the halo density and velocity dispersion profiles remains poorly understood.

Another well known result inferred from N-body simulations is that, in all the cosmologies investigated, the halo concentration $c = r_s / R$ decreases with increasing halo mass. NFW proposed that this is a consequence of the fact that, in hierarchical cosmologies, more massive halos form later when the mean density of the universe is lower. They demonstrated that the empirical mass-density relation is automatically recovered when the proportionality $c / (t_f)$ is assumed. They were forced, however, to define the formation time t_f as the time some progenitor collected one hundredth of the final halo mass. Salvador-Sole, Solanes, & Manrique (1998, hereafter SSM) showed, nonetheless, the robustness of that result using a better-motivated definition of the halo formation time: the last time the system was rearranged in a major merger. They also showed that the relation $c / (t_f)$ (strictly with t_f instead of t_f , though this makes no difference for the typical halo formation times in any popular cosmology) is equivalent to a universal dimensionless density profile for newborn halos, thus bringing some physical motivation to the assumed proportionality. Unfortunately, the z -dependence of the concentration predicted by such an assumption is not corroborated by N-body simulations (Bullock et al. 2001, hereafter B01).

A more promising result found by Avila-Reese, Firmani, & Hernandez (1998) was that the density profile of halos that have not been subjected to any major merger is very similar to the NFW profile. As discussed below, the continuous aggregation of small clumps proceeds essentially as secondary infall. It is therefore well understood why, using the spherical infall model from quite a realistic density profile of the initial perturbation such as the typical density run around peaks, Del Popolo et al. (2000) also found a density profile similar to the NFW one. On the other hand, since halos grow inside-out during secondary infall, these results are also consistent with the finding by Nusser & Sheth (1999) and Kull (2000) that the density profile of halos growing inside-out (or through stable clustering as the former authors call this process) and having not experienced a major merger is similar to the NFW profile.

However, the density profiles obtained from spherical infall do not satisfy the correct mass-concentration relation: the predicted concentration is substantially higher than that of simulated halos. Therefore, the role of spherical infall in the density profile of halos is still debatable. In this one respect, is also important mentioning that the inside-out growth condition is inconsistent with the dynamical effects of intermediate mass captures as small-size clumps tend to migrate to the halo center. Syer & White (1998) have examined the possibility that the NFW profile results from the repeated action of this kind of captures, concluding that it might explain the central cusp (see also Subramanian, Cen, & Ostriker 2000). But, as shown by Nusser & Sheth (1999), when the specific effects of intermediate captures are taken into account, the resulting density profile deviates more from the NFW profile than

the one obtained under strict accretion | the role, in this scheme, of the tidal stripping of captured clumps has been also examined by Dekel, Devor, & Hetzroni (2003); Dekel et al. (2003). Thus, before spherical infall can be considered as the main responsible for the density profile of halos, it is necessary to understand why the alterations induced by intermediate captures do not show up more frequently.

More importantly, all these works do not take into account the dramatic effects of major mergers (or fast accretion). By definition, this process causes the rearrangement of the system destroying in this way the density profile developed until that moment by spherical infall. Of course, this would go unnoticed if the density profile emerging from violent relaxation turns out to be very similar to the one a halo of the same mass would have developed through spherical infall. Surprisingly enough, numerical simulations indicate that this is just what happens. Indeed, high-resolution N-body simulations show that "the occurrence of a recent [major] merger is not an important factor affecting the [shape and the] concentration" of simulated halos (W02, p. 568). Likewise, the phase space density, $\langle r \rangle = \langle r^3 \rangle$, of halos in simulations of hierarchical cosmologies is found to follow, independently of their assembly history, a power-law for more than two decades in radius with logarithmic slope close to that predicted by Bertschinger (1985) using the spherical infall model (Taylor & Navarro 2001). Furthermore, the density profile of halos obtained in numerical simulations of monolithic collapse are very similar to those obtained in hierarchical cosmologies, which indicates that "the merger history does not play a role in determining the halo structure" (Moore et al. 1999, p. 1147; see also Huzz, Jain, & Steinmetz 1999a). In other words, the density profile of simulated halos is always the same regardless of whether (and when) their structure has been rearranged by major mergers. This necessarily implies that the density profile emerging from violent relaxation must be very similar to that developed through spherical infall. But what is the reason for such a coincidence?

The present paper attempts to answer all these questions. We begin in x 2 by describing the basic equations of a variant of the extended Press-Schechter (PS) model that are used in the computations of subsequent sections. We then examine, in x 3, whether pure accretion, which yields density profiles of the NFW type, can recover the mass-concentration relation of simulated halos. In x 4, we analyze the effects of mergers and intermediate captures. The results are summarized and discussed in x 5.

2. mass growth through accretion and mergers

The Modified Press-Schechter (MPS) model (SSM; Raig, Gonzalez-Casado, & Salvador-Sole 1998, and 2001, hereafter RGS) is a variant of the extended PS model intended to describe not only the mass growth of dark-matter halos in hierarchical cosmologies, but their inner structure as well. To this end it distinguishes between major and minor aggregation events (i.e., major and minor mergers or slow and fast accretion) according to whether they cause or not the complete rearrangement of the system, based on the usual comparison of the resulting fractional mass increase with respect to the reference halo with some pre-established threshold, η , separating the two

regimes. Note that a given aggregation event may be seen as a major or minor depending on the partner halo considered. For consistency, we say that halos are destroyed in major aggregation events while they survive in minor ones. We will follow here the most usual notation adopted in observational studies (and in SSM) and refer to major aggregation events as "mergers" and to the continuous aggregation of small clumps as "accretion" (one should avoid confusion with the different meaning of these words in other works; x 1).

According to the definition of η , the accretion rate, that is, the rate at which halos with M at t increase their mass between two mergers, is

$$r^a(M; t) = \int_{M^0}^{M(1+\eta)} r_{LC}(M'; M^0; t) dM^0; \quad (3)$$

with $r_{LC}(M'; M^0; t) dM^0$ the instantaneous transition rate at t from halos with M^0 to halos between M^0 and $M^0 + dM^0$, provided by the extended PS model (Lacey & Cole 1993)

$$r_{LC}(M'; M^0; t) = \frac{p}{2(M^0)} \frac{d_c d(M^0)}{dt} \frac{1}{1 - \frac{2(M^0)}{2(M)}} \exp \frac{\frac{2}{c}(t)}{2^2(M^0)} \frac{1}{1 - \frac{2(M^0)}{2(M)}} : \quad (4)$$

In equation (4), $d_c(t)$ is the linear extrapolation to the present time t_0 of the critical overdensity of primordial fluctuations collapsing at t , and (M) $(M; t_0)$ is the rms fluctuation of the density field at t_0 smoothed over spheres of mass M . Both $d_c(t)$ and (M) depend on the cosmology. The $M(t)$ track followed, during accretion, by halos with M_i at t_i is therefore the solution of the differential equation

$$\frac{dM}{dt} = r^a(M(t); t) \quad (5)$$

for the initial condition $M(t_i) = M_i$. Strictly speaking, this is the average track followed by those halos. Real accretion tracks actually differ from it owing to the random effects of individual captures. The scatter remains nonetheless quite limited along the typical lifetime of halos (see RGS).

The destruction of a halo does not necessarily imply the formation of a new one: the largest partner participating in the merger can perceive it as minor and survive. Only those mergers in which all initial halos are destroyed or, equivalently, none of them survives do mark the formation of a new halo. (The definitions of halo destruction and survival imply, indeed, that there is at most one surviving halo in any aggregation event.) Thus, the formation of a halo corresponds to the last time the system was rearranged in a merger.

To derive the formation rate we need to introduce the capture rate, $r^c(M^0; M; t) dM$, giving the rate at which a halo with mass M^0 at t results from a major merger of a halo with mass M to $M + dM$

$$r^c(M^0; M; t) dM = r_{LC}(M; M^0; t) [M^0 - M(1 + \eta)] \frac{N(M; t)}{N(M^0; t)} dM dt; \quad (6)$$

with $r_{LC}(M; M^0; t)$ given by equation (4), $N(M; t)$ the PS mass function, and $\eta(x)$ the Heaviside function. As shown by RGS, mergers leading to the formation of new

halos are essentially binary. This is consistent with the fact that the capture rate is closely symmetrical around $M = M^0/2$ (see Fig. 1 in RGS), at least in the range $M^0/m = (1 + m)/M^0 = (1 + m)$ corresponding to captures leading to the formation of new halos. Note that a fractional mass relative to the initial object equal to m represents a fractional mass relative to the final object equal to $m = (1 + m)$. Since each symmetrical pair of such captures produces the formation of one new halo with mass M^0 , the formation rate of halos of this mass is

$$r^f(M^0; t) = \frac{1}{2} \int_{M^0/m = (1 + m)}^{Z_{M^0/(1+m)}} r_{LC}(M; M^0; t) \frac{N(M; t)}{N(M^0; t)} dM : \quad (7)$$

The probability distribution function (PDF) of formation times can then be derived by taking into account that the mass evolution of a halo since its formation is given by the accretion track $M(t)$ solution of equation (5). Thus, the cumulative number density of halos at t_i with masses in the arbitrarily small range M_i to $M_i + M_i$ that pre-exist at a time $t < t_i$ or, equivalently, the spatial number density of halos that evolve by accretion from t to t_i ending up with a mass between M_i and $M_i + M_i$ is

$$N_{pre}(t) = \int_{t_i}^{Z_{t_i}} N(M_i; t_i) M_i \exp \left[- \int_t^{r^f(M(t^0); t^0)} r^f(M(t^0); t^0) dt^0 \right] dt^0 : \quad (8)$$

Consequently, the PDF of formation times for halos with masses between M_i and $M_i + M_i$ at t_i is given by

$$f(t|M_i) = \frac{1}{N(M_i; t_i) M_i} \frac{dN_{pre}}{dt} \Big|_{Z_{t_i}} = r^f(M_i; t_i) \exp \left[- \int_t^{r^f(M(t^0); t^0)} r^f(M(t^0); t^0) dt^0 \right] : \quad (9)$$

The median for this distribution defines the typical halo formation time.

The validity of all preceding analytical expressions was checked against numerical simulations in RGS. The fact that the simulations performed by Lacey & Cole (1994) used in that comparison have low resolution by today standards should not affect the conclusions drawn in RGS as they refer to the way halos grow and not to their inner structure. However, it is worth re-examining, now with the help of high-resolution simulations, the correct behavior of the mass accretion rate (eq. [3]) determining the density profile of halos in the present model (see next section).

In Figure 1, we compare the accretion histories predicted from the MPS model with those obtained by W02 from the high-resolution simulations of B01. The accretion histories of W02 have been converted to the definition of halo mass used in the present work (see x 3 for the values of f and u adopted). Note also that since the latter accretion histories include both major and minor aggregations they must be compared with our theoretical predictions drawn from equation (3) for m equal to unity. As can be seen, there is good agreement between theory and simulations. Only for halo masses above the critical mass for collapse, M_c , there is an increasing departure. This seems to reflect the difficulty of the PS formalism to correctly model the mass growth of halos towards large masses (see, e.g., Monaco 1997), although no such departure is detected in Fig. 3 of RGS.

3. the density profile set by accretion

The rearrangement, through violent relaxation, of a halo at its formation produces a more or less spherical system with a new density profile independent of the past history of the halo. On the other hand, accretion consists of frequent multiple captures of very small halos. Thus, the graininess of accreted matter can be neglected in a first approximation. The resulting configuration (i.e., a central relaxed spherical object surrounded by a rather smooth distribution of matter falling into it) approximately satisfies the conditions met in secondary infall. Consequently, halos grow inside-out during accretion, making it possible to determine the growth of their density profile from the accretion rate derived in the preceding section.

3.1. Predictions at $z = 0$

Consider a halo with current mass M having formed at t_f . During the subsequent accretion phase, the halo follows the $M(t)$ track solution of the differential equation (5). According to the inside-out growth condition, the mass accreted at any moment t is deposited at the instantaneous radius $R(t)$ of the system without altering the inner density profile. Consequently, we have

$$M(t) - M_f = \int_{R_f}^{R(t)} 4 \pi r^2(r) dr ; \quad (10)$$

with M_f and R_f the mass and radius at formation and (r) the density profile developed since that moment. By differentiating equation (10) and taking into account the definition of the virial radius

$$R(t) = \frac{3M(t)}{f^4 u(t)}^{1/3} \quad (11)$$

and equation (5), we are led to the expression

$$(t) = f_u(t) \left[1 - \frac{M(t)}{r^a M(t)} \frac{d \ln u}{dt} \right]^{1/3} \quad (12)$$

giving the density at $r = R(t)$. Equations (11) and (12) therefore define, in the parametric form, the density profile developing by accretion from the initial seed at t_f , at any radius $r = R_f$. Notice that, owing to the aforementioned dispersion of real $M(t)$ tracks around the solution of equation (5), the previous theoretical profile represents, like the NFW profile, the average density profile of halos with M at t , with individual profiles fluctuating around it.

The shape of this theoretical profile depends on the values of f and u entering the definition of the virial radius (eq. [11]). The need to choose appropriate values for these two quantities in order to obtain good predictions from the PS model is not new. For instance, the conditional as well as the unconditioned mass functions of halos showing a given abundance depend on the radius adopted to define the halo mass. In Figure 2, we plot the theoretical density profiles predicted from $u = u_{crit}$ and $u = u_{max}$ at $M = 0.25$ CDM cosmology assuming that accretion operates from a very small seed. As can be seen, $u = u_{crit}$ leads to a monotonous decreasing density profile, while $u = u_{max}$ leads to a density profile which tends to a level at those radii corresponding to cosmic times when becomes dynamically dominant. Since such radial behavior

is not observed in real or simulated halos, we conclude that the best value of u to use is u_{crit} . The resulting profile can then be further truncated, of course, at any smaller radius if necessary. This will be done when comparing our theoretical profile with the NFW profile that uses $u = u_{\text{crit}}$. Concerning f , the theoretical density profile is little sensitive to it, any usual value yielding similar results. Accordingly, unless we state otherwise, we will use $f = 200$ as in NFW.

The theoretical density profile also depends (through eq. [3]) on the value of m , the effective threshold for mergers. As explained in RG S, the comparison between theory and simulations in terms of halo masses alone puts no constraint on this parameter. In contrast, the inner structure of halos can be used to fix the value of this parameter. In Figure 3, we show the effects of varying m within the range $[0.3, 0.7]$ around the best value of 0.5 (see below), which we use hereafter.

Once the values of m , u , and f have been fixed, the theoretical density profile of halos with M at t having evolved by accretion from the initial seed formed at the last major merger can be inferred from equations (11) and (12). In Figure 3, we show the profiles obtained assuming pure accretion, meaning that the last major merger leading to the formation of the halo took place long ago, and we compare them to the corresponding NFW profiles. We plot only three cosmologies, although similar results are obtained in any of the cosmologies studied by NFW. Taken as a whole, there is a good agreement between the theoretical and empirical profiles down to $r = 10^{-2}R$ for halos spanning at least four decades in mass. However, a systematic tendency is observed for the accordance to worsen beyond M , becoming substantial at about $10 \text{ times } M$. This departure is likely caused by the above-mentioned deviation for large halo masses between the accretion histories predicted by the MPS model and those obtained in high-resolution simulations. But the most massive halos are scarce and seldom virialized (typically they have formed recently), so the disagreement between our model and the data is not important in practice.

Both the theoretical and empirical profiles shown in Figure 3 for different halo masses are completely fixed in shape as well as in scale. This means that our approach yields not only a density profile similar to the NFW one (at least for moderate and small halo masses), but also good values of c . In this respect, it is worth noting that the NFW expression is a fit, i.e., only a good approximation to the real density profile of simulated halos, and that the empirical mass-concentration relation is inferred from a small number of halos of different masses in each cosmology (the few points in the mass-concentration diagram in Fig. 5). This affects, of course, the comparison between the theoretical and empirical halo profiles performed in Figure 4. Hence, to better assess the quality of the predictions of our formalism it is preferable to adjust, through m minimization, the theoretical profiles corresponding to different halo masses by the NFW expression, as if they were the profiles of individual simulated halos, and compare the resulting theoretical mass-concentration relation with N -body data.

As shown in Figure 5, the theoretical mass-concentration relations above $10 M_{\odot}$ deviate strongly from the empirical data, particularly for power-law spec-

tra. As indicated by the χ^2 values, this departure is due to the progressive disagreement between the theoretical profile and the NFW expression with increasing halo mass. In contrast, below $10 M_{\odot}$, the empirical mass-concentration relationships for the cosmologies studied by NFW are well bracketed for m between 0.3 and 0.7, with the lower and upper bounds tending to yield too large and too small concentrations, respectively. Hence, were the effective frontier between accretion and mergers lowered to exclude intermediate captures, the predicted concentration would be larger than that found in simulated halos, in agreement with the results of Nusser & Sheth (1999), Kull (2000) and DelPopolo et al. (2000). In $\times 4$ we will provide, however, justification for the classification of intermediate captures as accretion.

3.2. Other redshifts

Since our model can be applied to any redshift, we can also derive the redshift dependence of c for halos of a fixed mass and compare it to that found by B01 in N -body simulations of the CDM cosmology. These authors adopted a halo radius R defined according to equation (11) with $u = u_{\text{crit}}$ as here, but f varying from 337 to 178 as z shifts from 0 to 5 according to the top-hat collapse model in the CDM cosmology. Therefore, in order to carry out this comparison one can derive the theoretical profile using $f = 200$ as above, and then truncate or extend it to the same z -dependent radius as in B01 or, alternatively, one can take advantage of the fact that the theoretical profile is little sensitive to f and derive it directly using the same $f(z)$ of B01. In the former case, the halo mass can only be known *a posteriori* after the appropriate truncation or extension of the halo density profile, while, in the latter case, it coincides with the mass used by B01. For this reason, we have chosen to follow the latter approach.

In Figure 6 we show the predicted $c(z)$ relation and compare it to that found by B01 for a halo mass equal to $5.55 \times 10^{12} M_{\odot}$, the central logarithmic value of the mass range $2.14 \times 10^{11} \text{ to } 1.43 \times 10^{14} M_{\odot}$ studied by these authors. This mass is small enough, along the whole range of redshifts involved in the comparison, for the theoretical profile to always be well adjusted by the NFW expression while, at the same time, it is sufficiently large to guarantee that simulated halos have a large number of particles and, hence, that their concentration is well determined. The agreement between the predicted and empirical $c(z)$ relations is good. We want to stress that this is the first correct prediction of $c(z)$ made by a physical model. Previous predictions based on the proportionality $c \propto u(t_f)$ proposed by NFW (corresponding to a universal dimensionless density profile of halos at formation; SSM) have been proved, on the contrary, not correct regardless of the exact definition of t_f used (see Fig. 6), while other analytical expressions which correctly fit the empirical function $c(z)$ are but toy models (B01; Eke, Navarro, & Steinmetz 2001).

What is wrong then with the assumption $c \propto u(t_f)$? According to the present model, all halos lying, at different epochs, along a given accretion track $M(t)$ have the same density profile, though truncated at their respective virial radii. The fact that the theoretical density profile of halos at $z = 0$ is reasonably well fitted by the NFW ex-

pression over the whole radial range implies that all those halos have essentially the same values of the scale parameters c and r_s (though not of c , which varies with z owing to the time dependence of R). In other words, c and r_s do not change along accretion tracks. Consequently, they remain constant for halos evolving by accretion (in agreement with the results of N -body simulations; Zhao et al. 2003). In particular, the value of c does not depend on the formation time of halos, but on their (last) accretion track.

4. the effects of mergers and intermediate captures

The preceding theoretical profile has been derived assuming pure accretion and the inside-out growth of halos during such a process. This presumes: 1) that halos have not undergone any merger for a very long period of time and 2) that the capture of clumps with intermediate masses has a negligible contribution in the accretion process. But both conditions are far from realistic in hierarchical cosmologies. For instance, N -body simulations (Tormen 1997) show that the average numbers of aggregations producing, in the standard CDM cosmology, a fractional mass increase in halos of cluster scale above 0.1, 0.2, and 0.5 along the age of the universe are, respectively, 13.7 14, 7.4 1.0, and 2.3 0.5. These values reduce to 2.7 0.5, 1.5 0.4, or 0.1 0.1 if we only consider the time elapsed since the formation of the halos, defined as in the original extended PS model, i.e., the time that half the mass of the halo was first collected in some progenitor (Lacey & Cole 1993), while our definition of halo formation time (see x 2) leads to intermediate values.

4.1. Mergers

Though rare, mergers are actually frequent enough to invalidate the assumption of pure accretion. This is illustrated in Figure 4. Arrows mark the radii of the seeds formed at the typical last merger of halos inside which the density profile predicted assuming pure accretion should be replaced by that yielded by violent relaxation. However, as mentioned in x 1, the latter profile is eventually very similar to the one the system would have developed through pure spherical infall. We want to emphasize that this is not a consequence of our modeling but an empirical fact drawn from high-resolution cosmological simulations. As shown next, such a "coincidence" emanates from the fact that violent relaxation takes some finite time to proceed during which accretion keeps going on. The final density profile then adopts the unique inner structure compatible with the boundary conditions imposed by the accreting layers.

We begin by showing first that the velocity dispersion profile (r) of halos in the outer accreted region is uniquely determined. It could be derived, of course, from the Jeans equation (2) provided we knew the value it takes at some given radius. But this is information that we do not have a priori (we are avoiding any unjustified assumption at infinity). What we only know is that the velocity dispersion profile of seeds emerging from violent relaxation in real non-isolated systems deviates from the uniform one expected for ideal isolated systems owing to the boundary conditions imposed by the infalling matter. This suggests

the following iterative way to determine the value of σ at $r = R_f$, the frontier between the inner seed and the outer accreted region.

The zero-order solution of σ^2 at $r = R_f$ is given by the squared value of the uniform velocity dispersion that violent relaxation tends to establish, given by equation (2) with null logarithmic derivative of σ^2 and logarithmic derivative of ρ corresponding to the known outer density profile. But violent relaxation takes a finite time to proceed, during which the instantaneous radius of the halo shifts outwards. Consequently, the same condition will hold at the new edge of the system after some arbitrarily small time. We can therefore derive in the same way the zero-order value of σ^2 at this new edge of the system. Those two values of σ^2 can then be used to determine the zero-order logarithmic derivative of σ^2 at $r = R_f$ and, by substituting this derivative into the equation (2), to infer the first-order value of σ^2 at that point. This iterative procedure rapidly converges to the wanted value of $\sigma^2(R_f)$.

Once we know the value of $\sigma(R_f)$, we can infer the velocity dispersion profile in the outer accreted region where the density profile is known (eqs. [11] and [12]) from the Jeans equation (eq. [2]). But this velocity dispersion profile must coincide with the one that can be obtained by directly applying the previous iterative procedure at any point of the outer region as both solutions satisfy, by construction, the Jeans equation for the same density profile and have identical values at R_f . To sum up, thanks to the uniform velocity dispersion profile that violent relaxation tends to establish in the inner seed, the velocity dispersion profile emerging in the outer accreted region is fully determined, turning out to be also as close to uniform as allowed by the density run there. In Figure 7, we compare, for the same halo masses and hierarchical cosmologies as in Figure 4, the velocity dispersion profile of simulated halos (Cole & Lacey 1997) with the theoretical one inferred following the previous iterative procedure over the whole radial range as would correspond to the case of pure accretion. As can be seen, the agreement between the theoretical and empirical velocity dispersion profiles is as good as in the case of the density profiles.

We can now proceed with our reasoning and focus on the density profile of the inner seed. Since violent relaxation lasts for some time during which matter is continuously falling into the halo, the total mass distribution adapts to the boundary conditions imposed by this matter infall. Thus, it must be in steady state, compatible with the shell crossing of infalling layers, and with a velocity dispersion as close to uniform as possible. But these are the same conditions satisfied by the halo during the accretion process. It is therefore well understood why the density profile emerging from a major merger coincides with the profile that would have developed by means of pure accretion. Furthermore, since the concept of orbital decay is meaningless during violent relaxation, there is no difference between intermediate and small captures during that process apart from the distinct mass increase they produce. Therefore, intermediate captures must be included in the formal accretion rate leading to the same density profile as violent relaxation.

It might be argued that the previous reasoning presumes

that violent relaxation proceeds to completion, while the relaxation time, equal to, say, three crossing times of the system at the time of the major merger,

$$t_{\text{rel}}(t_f) = 3 \frac{2}{V_c(t_f)} R(t_f) = 0.66 [G(t_f)]^{1/2}; \quad (13)$$

with $V_c = (GM/R)^{1/2}$ the circular velocity of the halo, is long enough for that condition not always to be satisfied. However, the NFW expression describes the average profile of halos having a relaxed appearance. That is, those halos observed before violent relaxation has gone to completion are not taken into account.

4.2. Intermediate Captures

Provided that halos do not undergo intermediate captures after the completion of violent relaxation at their last major merger, their density profile will develop inside-out as explained in §3. Strictly, there is no need, in the present case, for accretion to include intermediate captures, although given that the outermost profile is quite insensitive to the value of m used (see Fig. 3) this makes almost no difference in practice. If, on the contrary, halos undergo intermediate captures in such a late phase, as one would naively expect from the larger frequency of intermediate captures as compared to major ones, the density profile will become cusplike and deviate from the NFW profile.

What is therefore crucial to understand the shape of the NFW profile of relaxed halos is to see that such intermediate captures are quite improbable. This is not in contradistinction with the relatively high average numbers quoted by Tormen (1997). Here we must only consider those intermediate captures restricted to occur after the completion of the violent relaxation of the halo accompanying its last merger and early enough for the captured clump to have completed its orbital decay by the time the halo is observed. This latter bound is necessary, indeed, to guarantee that the halo does not show any substructure and can then be identified as a relaxed system. The low frequency of intermediate captures subject to these two constraints seems to be supported by the results of N-body simulations (Arago et al. 2002).

Let us therefore calculate the probability $P(M)$ that the last intermediate merger of a halo with M at t occurred after the completion of violent relaxation and the time at which the eventual intermediate merger should take place for the merged clump to reach the halo center by the time the halo is observed. This probability is given by

$$P(M) = \int_{t_0}^{t_f} \int_{t_{\text{fric}}(t)}^{t_f} \int_{m \text{ in } (t_f)}^{m = (1 + \frac{1}{m})} d\frac{d}{dt} M(t) dt_f dt; \quad (14)$$

with the integrand giving the joint probability that the halo was formed from t_f to $t_f + dt_f$ and underwent the last intermediate merger with a clump of instantaneous fractional mass between m and $m + dm$ in the infinitesimal interval of time around t . This joint probability is simply equal to the product of the probabilities $(dt_f M) dt_f$, given in equation (9), and $P_{\text{last}}(m; t_f M) dm$, calculated in the Appendix.

In equation (14), $t_f + t_{\text{rel}}(t_f)$ is the time of completion of violent relaxation after the last major merger at t_f ,

with the relaxation time t_f given by equation (13), and $t_0 = t_{\text{fric}}(t_0)$ is the time at which the intermediate merger should occur for the clump to have reached the halo center at t_0 . The characteristic time of orbital decay of a clump of mass M_s in a circular orbit of radius r is (e.g., Binney & Tremaine 1987)

$$t_{\text{dec}}(r) = \frac{r}{\frac{1}{0.43 \ln M(r) = M_s]} \frac{V_c(r) r^2}{G M_s}; \quad (15)$$

with $V_c(r) = [GM(r)=r]^{1/2}$ the circular velocity at r . Hence, by integrating $t_{\text{dec}} dr$ under the approximation of a singular isothermal halo (for which the integral is analytical) from 0 to the radius of the initial orbit, $R(t)$, at the time t of the merger, we have an estimate of the time spent by the clump to spiral to the halo center owing to dynamical friction

$$\begin{aligned} t_{\text{fric}}(t; m) &= \frac{1}{0.43 \ln M(t) = M_s} \frac{V_c(t) R(t)}{2 G M_s} \\ &= \frac{0.13}{\ln(0.3)} [G(t)]^{1/2}; \end{aligned} \quad (16)$$

where $M(t)$ and $V_c(t)$ are, respectively, the total mass and circular velocity of the halo at the time of the merger. Thus, $t_{\text{fric}}(t_0)$ is given by the previous expression for a time solution of the implicit equation $t + t_{\text{fric}}(t; m) = t_0$. Note that in deriving equation (16), we have assumed, for simplicity, that M_s remains constant and equal to about 30% of the mass of the merged clump after the initial tidal stripping, i.e., $M_s = 0.3M(t)$, with the fractional mass increase of the halo relative to the final object. According to Dekel, Devor, & Hetzroni (2003), the mass of clumps is reduced to 30% of its initial value after their orbits have already achieved a substantial decay. But these authors assume clumps with a density profile steeper than the NFW one at large radii, which means that their clumps are more difficult to tidally strip than real ones. On the other hand, we expect the real orbits of merged clumps to be typically elliptical rather than circular as we are assuming here, which should diminish their time of orbital decay. However, this effect should be balanced by the fact that, in the elliptical case, clumps fall deeper in the halo at their pericenter and, hence, are more severely truncated by tides since the beginning.

The upper bound for in equation (14) is not $m = 0.5$ but $m = (1 + \frac{1}{m}) = 0.33$ since the fractional mass increase is relative to the mass $M(t)$ of the halo after the merger. The lower bound m_{in} is the value of yielding a characteristic time of orbital decay for the initial orbit (eq. [15] with $r = R(t)$), equal to $t_0 = [t_f + t_{\text{rel}}(t_f)]$, that is, the solution of the implicit equation

$$\frac{0.27}{\ln(0.3)} \frac{1}{m_{\text{in}}} \frac{1}{G f t_0} \frac{1}{[t_f + t_{\text{rel}}(t_f)] g} = t_0 = [t_f + t_{\text{rel}}(t_f)]; \quad (17)$$

Values of smaller than this limit correspond to clumps that do not suffer any significant orbital decay.

In Figure 8, we show, for different halo masses and cosmologies, the quantity P giving the probability that intermediate captures can affect the halo density profile that would emerge from the last major merger and the subsequent accretion phase, calculated in §3. As can be seen,

this probability decreases with increasing mass. It becomes negligible for halos more massive than about M in all cosmologies, but even for the smallest halo masses considered by NFW, equal to $10^{-2}M$ for CDM spectra or $10^{-1.5}M$ for power-law ones, it is quite small. Certainly, the exact values shown in this plot should not be taken too literally given that they depend on the exact definitions of t_{rel} and t_{frac} adopted. But it is equally true that equation (14) gives an upper bound for P since, in its derivation, it has been implicitly assumed that the mass increase in captures comes from one unique clump, while it might also be produced by two or more less massive clumps not falling then into the category of intermediate captures. What is more important, more than one intermediate merger is required to affect appreciably the density profile, while the probability that two or more intermediate captures take place in the right time interval is obviously much smaller.

5. summary and discussion

We have presented a simple analytical model for the density profile developed by halos during accretion based on their inside-out growth in that regime. The resulting density profile is found to be similar to the NFW profile in agreement with previous works. However, contrarily to these same works, we also find good agreement between theory and simulations concerning the mass-concentration relations of halos at $z = 0$. More importantly, our physical model correctly predicts the mass-concentration relation at any redshift. An analytical model such as the one presented here, able to make reasonable predictions on the density profile of halos at any epoch and in any cosmology, should be then very useful in the modeling of galaxy formation and evolution. Caution must be taken, however, in using the present model on halos more massive than $10M(t)$, with $M(t)$ the typical mass for collapse at t . For masses this large, the theoretical profile shows a substantial departure from the empirical one likely due to a deficient modeling of halo growth by the PS formalism at the large mass end.

The success of our model compared to previous ones appears to rely on the inclusion of intermediate-mass captures in the accretion regime despite the fact that they do not satisfy the inside-out growth condition. This is justified by the realization that the halo density profile is actually not set during accretion (except for the narrow outermost radial range, in logarithmic units), but at the time of the last major merger, both processes leading to halos with essentially the same shape. Given that there is no difference between the dynamical effects of minor and intermediate captures during the violent relaxation resulting from mergers, it is then understandable why intermediate captures must be included formally in the accretion process.

The fact that major mergers yield essentially the same density profile than pure accretion is an important result of high-resolution numerical simulations that has been pointed out only by a few authors (W02; Moore et al. 1999; Huzz, Jain, & Steinmetz 1999a). We have shown here that this unexpected coincidence is simply due to the unicity of the steady structure compatible with the boundary conditions imposed by the ever falling surrounding material. Thus, we have been able to reconcile the well-known result that pure accretion (or spherical infall) yields density profiles of the NFW form with the fact that, in hierarchical cosmologies, halos endure from time to time important mergers (or short periods of intense accretion) that bring them far from equilibrium and cause the rearrangement of their preceding structure. Besides, we have demonstrated that there is no time for intermediate captures to alter the density profile a la NFW established after the last merger without giving the halo a non-relaxed appearance.

Finally, we want to remark that our aim here was not to infer an accurate density profile for dark-matter halos, but to investigate its possible origin. For this reason we have considered the simplest case of pure dark-matter halos while, in the real universe, about 10–15% of the halo mass is in the dissipative baryonic component. This might have appreciable effects on the density profile of real systems. Likewise, we have assumed spherical symmetry and neglected halo rotation, as well as the possible anisotropy of the local velocity tensor. Real halos have, on the contrary, some angular momentum and are immersed in large filamentary structures making them accrete matter preferentially along one privileged direction (West 1994) and feel the tidal field of such anisotropic structures (Salvador-Sole & Solanes 1993). Moreover, even with perfect spherical symmetry, some velocity anisotropy will prevail in the halo outskirts, as observed, owing to the distinct evolution of the radial and tangential velocity dispersions of infalling layers. We note, however, that our density profile is independent of the actual degree of anisotropy of the velocity tensor.

We thank Guillermo González-Casado for helpful discussions and Julio Navarro for kindly providing the data of the mass-concentration relations. We also thank Julio Navarro, James Bullock, and their respective collaborators for making public the codes necessary to reproduce their results. This work was supported by the Spanish D.G.E.S. grant AYA 2000-0951. A.M. acknowledges the hospitality of the CIDA station in Merida (Venezuela) where part of this work was carried out.

APPENDIX

probability of the last intermediate merger

Let us consider the rate of intermediate captures up to some given fractional mass increase of halos with initial mass M^0 at t

$$r^i(M^0; \cdot; t) = \int_{M^0}^{Z_M(t)} r_{\text{LC}}(M; M^0; t) \frac{N(M; t)}{N(M^0; t)} dM : \quad (\text{A1})$$

Following the same reasoning leading to the PDF of formation times, but adapted to the previous range of intermediate

captures, we have that the cumulative number density of current halos with masses in the arbitrarily small range M to $M + dM$ that have undergone the last intermediate merger up to the present time is

$$N_{\text{last}}(M; t) = N(M; t_0) M \exp \int_{t_0}^t r^i M(t^0; t^0) dt^0 ; \quad (A2)$$

where $M^i(t)$ stands for the accretion track calculated using a modified threshold for mergers \sim_m corresponding to m to take into account that, on the final phase, accretion should not include intermediate captures. Hence, the PDF of times that halos with current mass M underwent their last intermediate merger yielding a fractional mass increase from M to $M + dM$ is simply

$$P_{\text{last}}(M; t) dM = \frac{1}{N(M; t_0) M} \frac{\partial^2}{\partial t \partial M} N_{\text{last}}(M; t) dt : \quad (A3)$$

REFERENCES

Arias, Y., Yepes, G., Gottlöber, S., & Müller, V. 2002, *ApJ* (submitted)

Avilá-Reese, V., Jiménez, C., & Hernández, X. 1998, *ApJ*, 505, 37

Bertschinger, E. 1985, *ApJS*, 58, 39

Binney, J., & Tremaine, S. 1987, *Galactic Dynamics* (Princeton: Princeton University Press)

Bond, J. R., Cole, S., Efstathiou, G., & Kaiser, N. 1991, *ApJ*, 379, 440

Bower, R. J. 1991, *MNRAS*, 248, 332

Bullock, J. S., Kolatt, T. S., Sigad, Y., Somerville, R. S., Kravtsov, A. V., Klypin, A. A., Primack, J. R., & Dekel, A. 2001, *MNRAS*, 321, 559 (B01)

Cohn, J. D., Bagla, J. S., & White, M. 2001, *MNRAS*, 325, 1053

Cole, S., & Lacey, C. 1997, *MNRAS*, 281, 716

Dekel, A., Devor, J., & Hertzroni, G. 2003, *MNRAS*, (in press)

Dekel, A., Arad, I., Devor, J., & Birnboim, Y. 2003, *ApJ*, (in press)

Del Popolo, A., Gambara, M., Recamier, E., & Spedicato, E. 2000, *A&A*, 353, 427

Engineer, S., Kannekar, N., & Padmanabhan, T. 2000, *MNRAS*, 314, 279

Filmore, J. A., & Goldreich, P. 1984, *ApJ*, 281, 1

Fukushige, T., & Makino, J. 2001, *ApJ*, 557, 533

Gott, J. R. 1975, *ApJ*, 201, 296

Green, J. E. 1977, *ApJ*, 218, 592

Green, J. E., & Gott, J. R. 1972, *ApJ*, 176, 1

Henriksen, R. N., & Widrow, L. M. 1999, *MNRAS*, 302, 321

Homan, Y., & Shaham, J. 1985, *ApJ*, 297, 16

Huss, A., Jain, B., & Steinmetz, M. 1999a, *ApJ*, 517, 64

Huss, A., Jain, B., & Steinmetz, M. 1999b, *MNRAS*, 308, 1011

Jing, Y. P., & Suto, Y. 2000, *ApJ*, 529, L69

King, I. R. 1972, *ApJ*, 174, L123

Kitayama, T., & Suto, Y. 1996, *MNRAS*, 280, 638

Klypin, A., Kravtsov, A. V., Bullock, J. S., & Primack, J. R. 2001, *ApJ*, 554, 903

Kull, A. 2000, *ApJ*, 516, L5

Lacey, C., & Cole, S. 1993, *MNRAS*, 262, 627

Lacey, C., & Cole, S. 1994, *MNRAS*, 271, 676

Lokas, E. L. 2000, *MNRAS*, 311, 423

Lokas, E. L., & Homan, Y. 2000, *ApJ*, 542, L11

Lynden-Bell, D. 1967, *MNRAS*, 136, 101

Monaco, P. 1997, *MNRAS*, 290, 489

Manrique, A., Salvador-Sole, E. 1996, *ApJ*, 467, 504

Moore, B., Governato, F., Quinn, T., Stadel, J., & Lake, G. 1998, *ApJ*, 490, 493

Moore, B., Quinn, T., Governato, F., Stadel, J., & Lake, G. 1999, *MNRAS*, 310, 1147

Navarro, J. F., Frenk, C. S., & White, S. D. M. 1996, *ApJ*, 462, 563

Navarro, J. F., Frenk, C. S., & White, S. D. M. 1997, *ApJ*, 490, 493 (NFW)

Eke, V. R., Navarro, J. F., & Steinmetz, M. 2001, *ApJ*, 554, 114

Nusser, A., & Sheth, R. K. 1999, *MNRAS*, 303, 685

Nusser, A. 2001, *MNRAS*, 325, 1397

Percival, W. J., Miller, L., & Peacock, J. A. 2000, *MNRAS*, 318, 273

Power, C., Navarro, J. F., Jenkins, A., Frenk, C. S., White, S. D. M., Springel, V., Stadel, J., & Quinn, T. 2003, *MNRAS*, 338, 14

Press, W. H., & Schechter, P. 1974, *ApJ*, 187, 425

Raig, A., González-Casado, G., & Salvador-Sole, E. 1998, *ApJ*, 508, L119

Raig, A., González-Casado, G., & Salvador-Sole, E. 2001, *MNRAS*, 327, 939 (RG S)

Ryden, B. S. 1988, *ApJ*, 333, 78

Ryden, B. S., & Gunn, J. E. 1987, *ApJ*, 318, 15

Salvador-Sole, E., & Solanes, J. M. 1993, *ApJ*, 417, 427

Salvador-Sole, E., Solanes, J. M., & Manrique, A. 1998, *ApJ*, 499, 542 (SSM)

Saslaw, W. C. 1987, *Gravitational Physics of Galactic and Stellar Systems* (ed with corrections; Cambridge: Cambridge University Press)

Shapiro, P. R., Iliev, I. T., & Raga, A. C. 1999, *MNRAS*, 307, 203

Somerville, R. S., & Kolatt, T. S. 1999, *MNRAS*, 305, 1

Taylor, J. E., & Navarro, J. F. 2001, *ApJ*, 563, 483

Tormen, G., Bouchet, F. R., & White, S. D. M. 1997, *MNRAS*, 286, 865

Tormen, G. 1997, *MNRAS*, 290, 411

Subramanian, K., Cen, R., & Ostriker, J. P. 2000, *ApJ*, 538, 528

Syer, D., & White, S. D. M. 1998, *MNRAS*, 293, 337

Wechsler, R. H., Bullock, J. S., Primack, J. R., Kravtsov, A. V., & Dekel, A. 2002, *ApJ*, 568, 52 (W02)

West, M. J. 1994, *MNRAS*, 268, 79

Zaroubi, S., & Homan, Y. 1993, *ApJ*, 416, 410

Zhao, D. H., Moore, H. J., Jing, Y. P., & Bomer, G. 2003, *MNRAS*, 339, 12

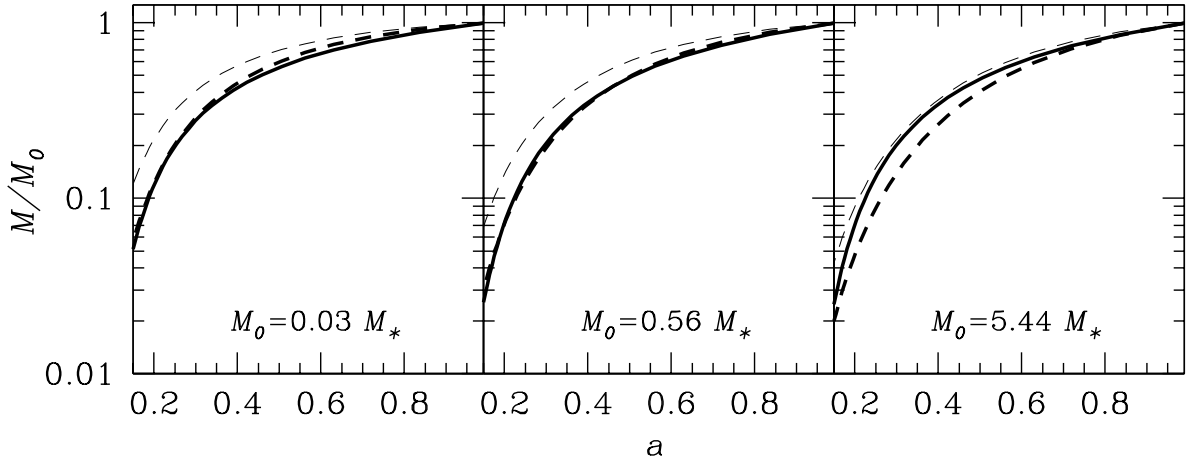


Fig. 1. Mass accretion histories for three halos in the Λ CDM cosmology studied by B01. The MPS predictions for m equal 1 (thick dashed lines) and 0.5 (thin dashed line) are compared to the analytical expression proposed by W02 to fit the mass accretion histories drawn from the N-body simulations of B01 (full line). $M = 2.39 \times 10^{13} M_\odot$ is the typical mass for collapse of density fluctuations at $z = 0$ for this cosmology.

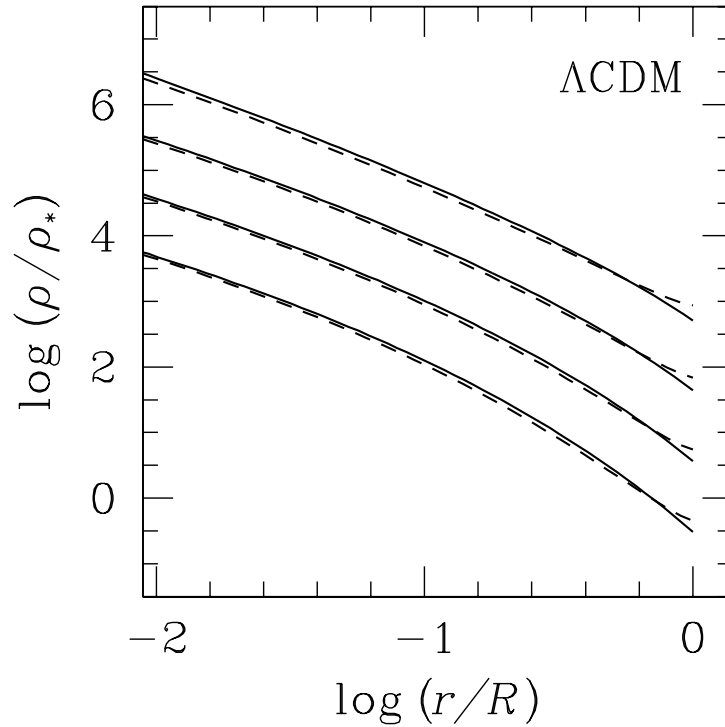


Fig. 2. Theoretical density profiles for halos at $z = 0$ with masses equal to $10^2 M_\odot$, $10^1 M_\odot$, M_\odot , and $10 M_\odot$ (from bottom to top) in a Λ CDM model inferred using $u = u_{\text{crit}}$ (dashed lines) and $u = u$ (solid lines). We are using the same cosmological parameters and delimitation of halos as in NFW and $m = 0.5$. M_\odot is the typical mass for collapse of density fluctuations and u stands for $u_{\text{crit}} M_\odot = M_\odot$.

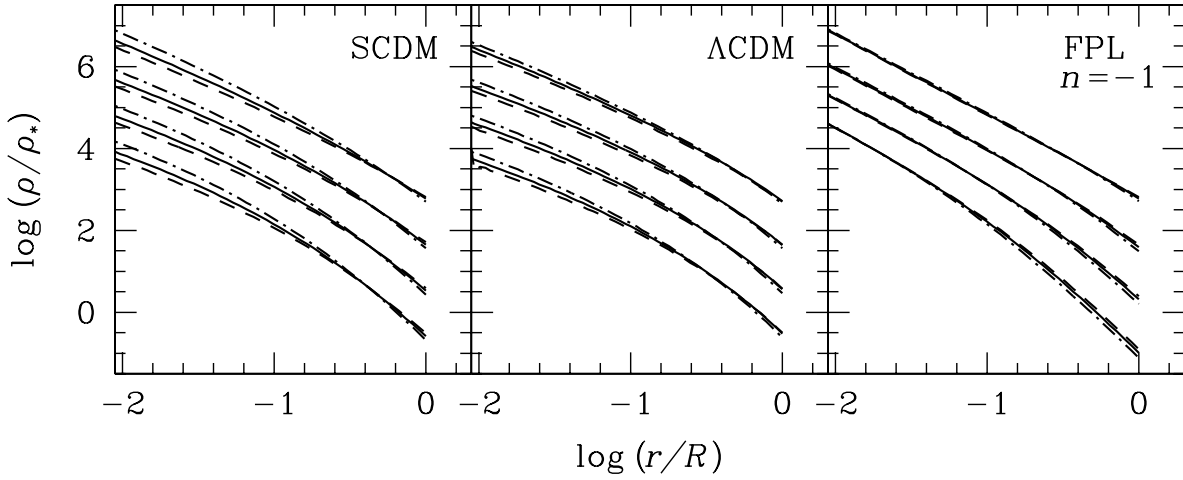


Fig. 3.1 Theoretical density profiles for halos at $z = 0$ with the same masses as Fig. 1 obtained for different values of the threshold for mergers: $m = 0.3$ (dot-dashed lines), 0.5 (solid lines), and 0.7 (dashed lines). The three cosmologies represented are at, Λ , Λ CDM model (SCDM), at, Λ , Λ CDM model (Λ CDM), and at, Λ , Λ model (FPL) with power-law spectrum of density fluctuations of index $n = -1$. All model parameters are the same as in the corresponding cosmologies of NFW.

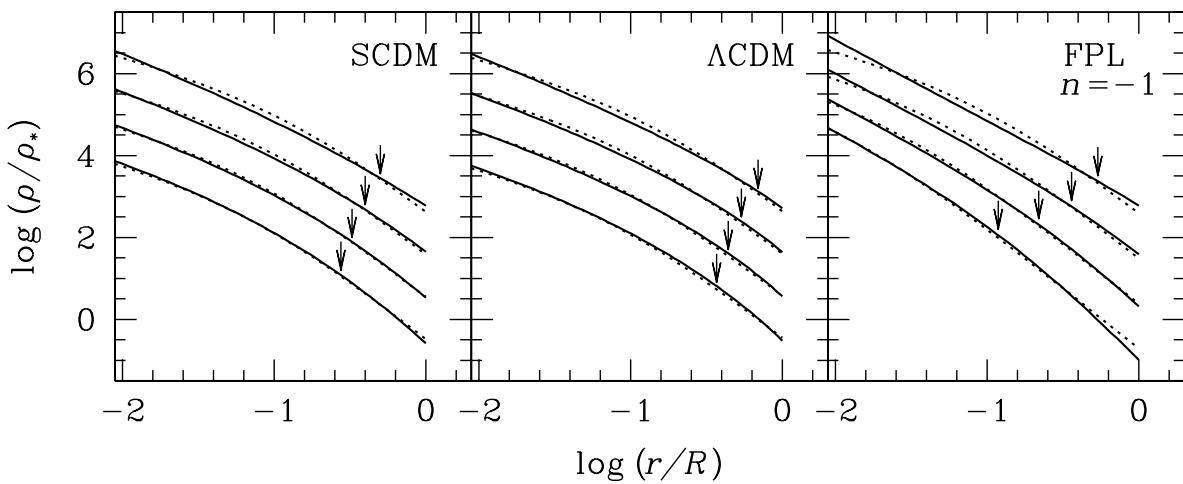


Fig. 4.1 Theoretical (solid lines) and NFW (dotted lines) density profiles for halos at $z = 0$ for the same masses used in the previous figures and the same cosmologies depicted in Fig. 2. Arrows mark the halo radii at the typical halo formation times.

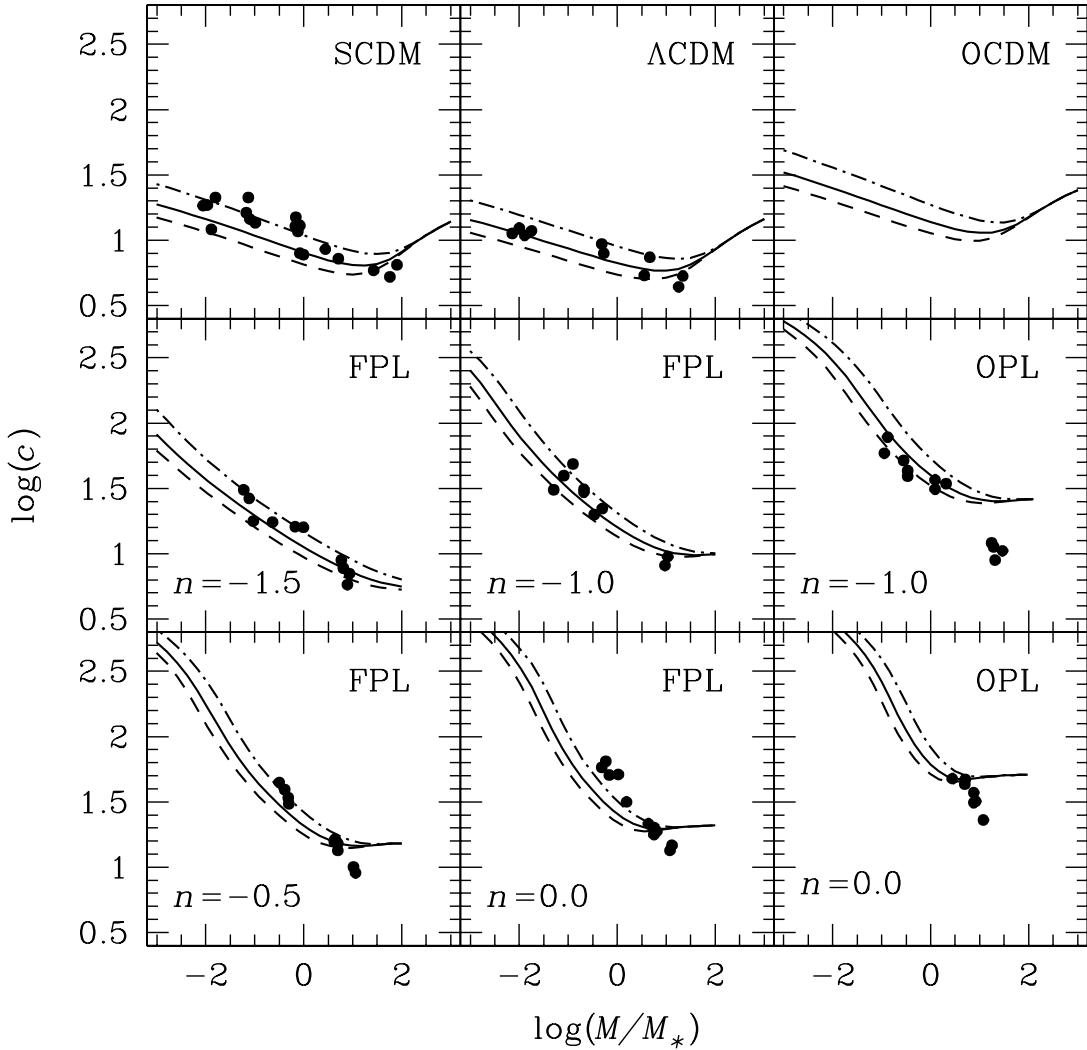


Fig. 5. Mass-concentration relation for halos at $z = 0$ obtained by fitting the theoretical density profiles derived in the present paper by the NFW analytical expression. The solid line corresponds to $m = 0.5$, while the dot-dashed and dashed lines correspond to the rather extreme values of 0.3 and 0.7, respectively. The dark points are those obtained by NFW from high resolution numerical simulations. We plot all the cosmologies studied by these authors, which, apart from those mentioned in the previous Figures, are two $m = 0.10$ power-law models (OPL) with $n = 0, 1$, and three more at $m = 0$, power-law models (FPL) with $n = 0, 0.5, 1.5$. We also show the predictions for an open, $m = 0.25$, CDM cosmology (OCDM), normalized as the CDM model, not included in the study by NFW.

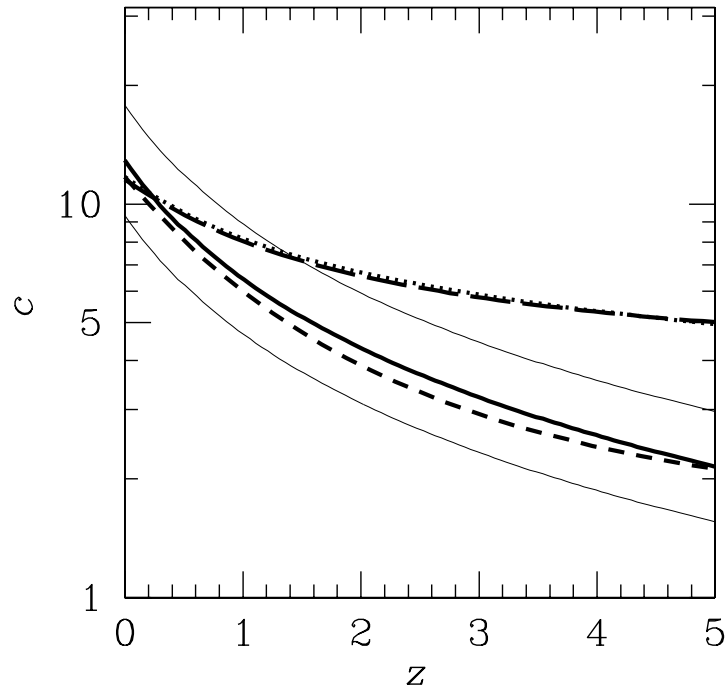


Fig. 6. Concentration vs. redshift in the CDM cosmology studied by B01 for a fixed halo mass M equal to $5.55 \times 10^{12} M_\odot$. The function proposed by B01 to fit their empirical data (solid line) and the corresponding intrinsic 68% spread (thin solid lines) are compared to our theoretical prediction (dashed line) and the $c(z)$ dependence suggested by NFW (long-dashed line) and SSM (dotted line).

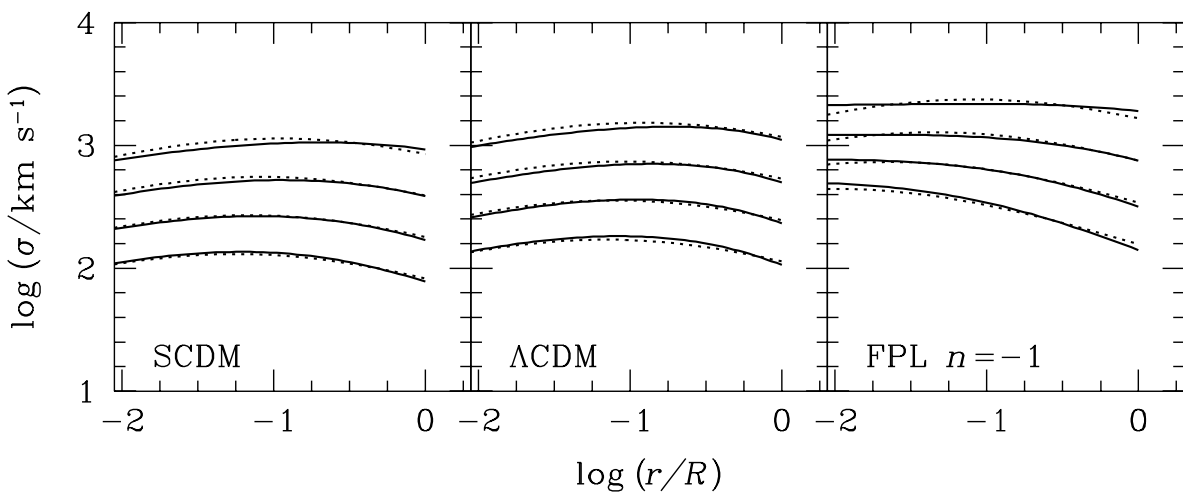


Fig. 7. Same as Fig. 3 but for the velocity dispersion profile.

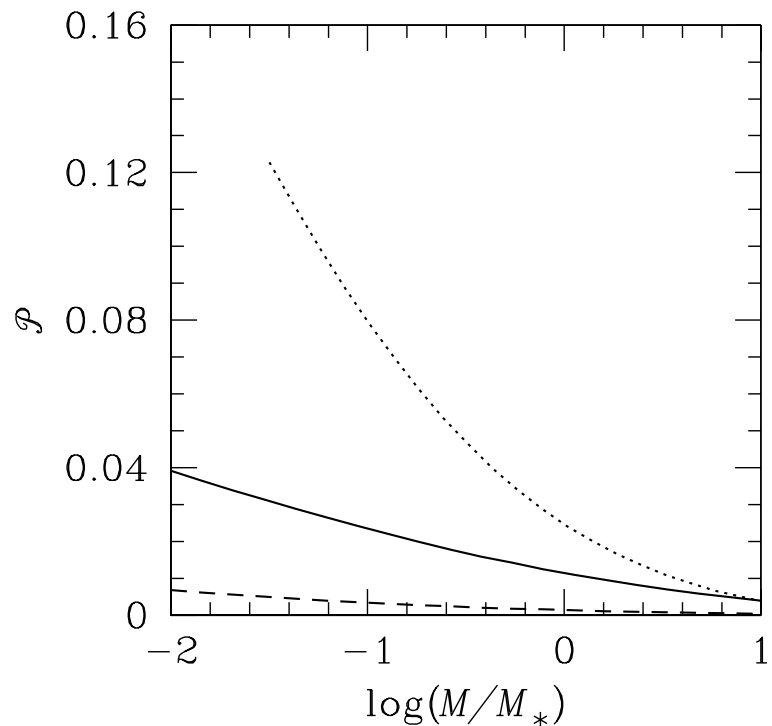


Fig. 8.] Probability that currently relaxed halos with mass M have undergone some merger with a clump of mass in the range required to modify the NFW-like profile arising from their last major merger and the subsequent accretion phase. The different curves correspond to the cosmologies plotted in Figs. 2, 3, and 7: SCDM (solid line), CDM (dashed line), and FPL $n = 1$ (dotted line).